APPLYING THE LANGMUIR-TYPE MASS TRANSPORT MODEL ON THE WATER ABSORPTION IN VEGETABLE FIBER REINFORCED POLYMER COMPOSITES: A FINITE-VOLUME APPROACH

Rafaela Q. C. Melo

rafaelaquinto@live.com

Department of Materials Engineering

Federal University of Campina Grande, 58429-000, Campina Grande, Paraíba, Brazil

Wanessa R. G. Santos

wanessa.raphaella@yahoo.com

Department of Mechanical Engineering

Federal University of Campina Grande, 58429-000, Campina Grande, Paraíba, Brazil

Antonio G. B. Lima

antonio.gilson@ufcg.edu.br

Department of Mechanical Engineering

Federal University of Campina Grande, 58429-000, Campina Grande, Paraíba, Brazil

Abstract. *This work presents an one-dimensional and transient mathematical modeling based on the Langmuir-Type Model to predict the moisture transport inside the composite materials. The numerical solution of the governing equation has been obtained using the finite-volume method, considering constant thermo-physical properties. Results of the moisture absorption kinetics and free and trapped water molecules concentration distribution, and moisture content distribution inside the material along the process are shown and analyzed. Predicted results compared to experimental data of average moisture content have shown that the model was effective for description of the phenomenon.*

Keywords: *Composites, Vegetable Fibers, Langmuir Model, Numerical Solution*

Proceedings of the XXXVIII Iberian Latin-American Congress on Computational Methods in Engineering P.O. Faria, R.H. Lopez, L.F.F. Miguel, W.J.S. Gomes, M. Noronha (Editores), ABMEC, Florianópolis, SC, Brazil, November 5-8, 2017.

1 INTRODUCTION

The use of vegetal fibers has presented great potential for technological application due to its potential as substitute of the synthetic fibers. The production of these fibers, presents a great socio-economic character, especially in Brazil, where they are produced by communities of the north and northeast regions. Their use as reinforcement in composite materials present advantages in terms of its low density, low cost, being obtained from renewable sources, are widely available and environmentally superior to synthetic fiber (Joshi et al., 2004; Cruz et al., 2010; Mohammed et al., 2015; Omrani et al., 2015; Patel et al., 2016).

The main disadvantage of these materials as reinforcement in polymer composites is their susceptibility to the influence of environmental agents, especially humidity. The effects caused by a long period of exposure to moisture may be irreversible due to the affinity of the water with specific functional groups of the reinforcements. High moisture absorption causes an increase in weight, a decline in mechanical properties and swelling of the fibers causing changes in the their shape and harming their application in projects that require greater dimensional accuracy. Thus, the prediction of the moisture content of the polymer composites reinforced with vegetable fibers is particularly important, since from the results obtained is possible to predict which areas are more susceptible to cracks and deformations that decrease the quality of the product under humid environments (Cunha et al., 2006; Carvalho et al., 2013; Mohammed et al., 2015).

The development of computational codes for diffusion problems allows obtaining by simulation, with speed and versatility, the optimal conditions of process and prediction of the areas susceptible to the degradation of the material. The numerical tools are adequate and reliable when is used the appropriate method to solve the governing equations and a mathematical model that faithfully represents the physical phenomenon. The widely adopted model for describing the mass diffusion process is based on the Fick's diffusion law, however, there are studies in the literature describing diffusive processes that do not follow this law, and further there are many sophisticated theoretical approaches to understanding the Non-Fickian diffusion. In this sense, Glaskova et al. (2012) have used the Langmuir diffusion model to describe the kinetics of water sorption. The model was initially proposed by Carter and Kilber (1978) and it is based on the hypothesis of the existence of probabilities describing two "states" of absorbed water. In the first state, the free molecules diffuse with concentration-independent diffusivity and are absorbed with a probability λ per unit time. In the second one, the molecules leave the trapped state and become free with a probability μ per unit of time. Therefore, the diffusion process is described by the same Fick equations, being modified only by the addition of these two parameters, which makes the Langmuir model more complete for the description of this phenomenon.

Thus, the objective of this work was to develop a transient and one-dimensional mathematical modeling and its numerical solution to predict mass transfer during water absorption in polymeric composite reinforced with vegetable fiber based on the Langmuir model. This study aims to contribute to the understanding of the effects and mechanisms of moisture migration, allowing engineers and researchers to take the correct decisions in the choice of materials for specific applications.

Proceedings of the XXXVIII Iberian Latin-American Congress on Computational Methods in Engineering P.O. Faria, R.H. Lopez, L.F.F. Miguel, W.J.S. Gomes, M. Noronha (Editores), ABMEC, Florianópolis, SC, Brazil, November 5-8, 2017.

2 MATHEMATICAL MODELING

2.1 The physical problem

For the physical model was considered a plate with thickness 2a, immersed in a fluid solute (water), placed in a container of thickness (2L + 2a) as pictured in Fig. 1. The moisture absorption was analyzed considering the following hypotheses: The material is considered homogeneous and isotropic; The diffusion coefficient is considered constant; The solid is considered symmetrical in relation to the center; The process is transient; There is not variation in the dimensions of the material during the diffusion process; Transport by capillary through the solid is considered negligible; Mass generation inside the solid not happens; The solid is totally dry at the beginning of the process, and finally the boundary condition is in equilibrium with the surrounding, at the surface of the solid.

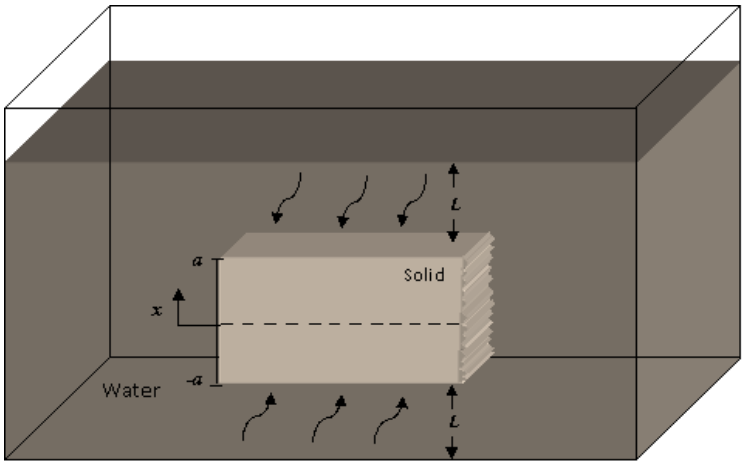

Figure 1 - Geometric representation for the physical model in an one-dimensional approach

2.2 The model

In the Langmuir model, the non-Fickian behavior of moisture absorption can be explained quantitatively by assuming that the moisture absorption consists of two phases, one free phase and the other trapped (Carter and Kilber, 1978).

The Langmuir equation written in cartesian coordinates is described as:

$$\frac{\partial C}{\partial t} = \frac{\partial}{\partial t}\left(\frac{D\partial C}{\partial t}\right) - \frac{\partial S}{\partial t} \tag{1}$$

where,

$$\frac{\partial S}{\partial t} = \lambda C - \mu S\,. \tag{2}$$

In Eq. (2), λ is the probability of free water molecules becomes trapped, μ is the probability of a trapped molecule becoming free, D is the diffusion coefficient of free molecules, C is the concentration of free molecules and S represents the concentration of the

molecules entrapped inside the material. For the proposed problem, the following initial and boundary conditions were considered:

- Inicial condition:

$$S = C = 0, -a < x < a, \quad t = 0 \tag{3}$$

- Boundary condition:

$$L\frac{\partial C}{\partial t} = -D\frac{\partial C}{\partial x}, x = \pm a, \quad t > 0 \tag{4}$$

where L represents the distance between the solid surface and the top or bottom of the water tank. According to Eq. (4), it is assumed that the solute rate leaving the solution is equal to the diffusive flux at the surface of the solid.

The absorption process continues until the number of molecules entrapped equals the number of free molecules (saturation equilibrium). Thus, the following equilibrium equation is satisfied:

$$\lambda C = \mu S \tag{5}$$

2.3 Numerical Solution: Finite-Volume Method

For the discretization of Eq. (1), the continuous solid of a thickness a was considered. Since the solid in question is symmetrical with respect to the center, it was subdivided in (np-1) control volumes, as shown in Fig. 2.

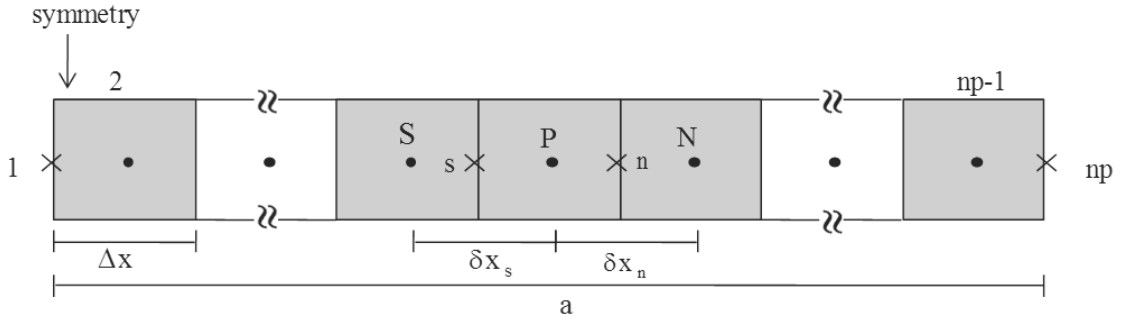

Figure 2. Representation of the simulation domain with (np-2) control volumes

In Fig. 2 each control volume has thickness Δx; S, P and N represent nodal points, while s and n represent the left and right faces of the control volume P; δx_s and δx_n represent the distance between nodal point P and nodal points S and N, respectively.

- Concentration of free solute

A) Internal points (3 to np-1 control volumes)

The Eq. (1) in terms of the variable Φ, can be written as follows:

$$\frac{\partial}{\partial t}(\zeta\Phi) = \frac{\partial}{\partial x}\left(\Gamma^{\Phi}\frac{\partial \Phi}{\partial x}\right) + S^{\Phi} \tag{6}$$

where, $\Phi = C$ represents the concentration of free molecules, $\Gamma^{\Phi} = D$ represents the mass diffusivity, S^{Φ} represents the source term and $\zeta = 1$.

The discretization process is done by applying the integral in all terms of Eq. (1) in volume and time, as follows:

$$\int_V \int_t \frac{\partial}{\partial t}(\zeta \Phi) dt dV = \int_t \int_V \frac{\partial}{\partial x}\left(\Gamma^{\Phi} \frac{\partial \Phi}{\partial x} \right) dV dt + \int_t \int_V S^{\Phi} dV dt \tag{7}$$

For an one-dimensional problem, we have that dV=dx, so Eq. (7) can be written as:

$$\int_x \int_t \frac{\partial}{\partial t}(\zeta \Phi) dt dx = \int_t \int_x \frac{\partial}{\partial x}\left(\Gamma^{\Phi} \frac{\partial \Phi}{\partial x} \right) dx dt + \int_t \int_x S^{\Phi} dx dt \tag{8}$$

Thus, after the integration process and using fully implicit formulation we obtain:

$$\left(\zeta_P \Phi_P - \zeta_P^o \Phi_P^o \right) \Delta x = \left[\Gamma_n^{\Phi} \left(\frac{\Phi_N - \Phi_P}{\delta x_n} \right) - \Gamma_s^{\Phi} \left(\frac{\Phi_P - \Phi_S}{\delta x_s} \right) \right] \Delta t + S^{\Phi} \Delta x \Delta t \tag{9}$$

Rearranging the terms of Eq. (9) in the linearized discrete algebraic form applied to the point P, we have:

$$A_P \Phi_P = A_N \Phi_N + A_S \Phi_S + A_P^o \Phi_P^o + B \tag{10}$$

where,

$$A_P = \left(\zeta_P \frac{\Delta x}{\Delta t} + \frac{\Gamma_s^{\Phi}}{\delta x_s} + \frac{\Gamma_n^{\Phi}}{\delta x_n} \right) \tag{11}$$

$$A_N = \left(\frac{\Gamma_n^{\Phi}}{\delta x_n} \right) \tag{12}$$

$$A_S = \left(\frac{\Gamma_s^{\Phi}}{\delta x_s} \right) \tag{13}$$

$$A_P^o = \left(\zeta_p \frac{\Delta x}{\Delta t} \right) \tag{14}$$

$$B = S^{\Phi} \Delta x = \left(\frac{S_P^o - S_P}{\Delta t} \right) \Delta x \tag{15}$$

The coefficients A_P, A_N and A_S represent the conductance between the nodal points P and their corresponding neighbors. The term A_P^o represents the influence of the value of Φ^o on the value of Φ at the current time. Equation (10) is valid for all internal points of the domain except for the boundary and symmetry points.

B) Symmetry points (control volume 2)

The discretized equation for the points of symmetry is obtained in a way analogous to Eq. (10). There is no flux on the left side due to symmetry, thus: $\Phi_P = \Phi_S$. Then, the Eq. (9) can be written as follows:

$$\left(\zeta_P \Phi_P - \zeta_P^o \Phi_P^o\right)\Delta x = \left[\Gamma_n^{\Phi}\left(\frac{\Phi_N - \Phi_P}{\delta x_n}\right)\right]\Delta t + S^{\Phi}\Delta x \Delta t \tag{16}$$

Rearranging the terms, we obtain the discretized equation for the points of symmetry as follows:

$$A_P \Phi_P = A_N \Phi_N + A_P^o \Phi_P^o + B \tag{17}$$

where,

$$A_P = \left(\zeta_P \frac{\Delta x}{\Delta t} + \frac{\Gamma_n^{\Phi}}{\delta x_n}\right) \tag{18}$$

$$A_N = \left(\frac{\Gamma_n^{\Phi}}{\delta x_n}\right) \tag{19}$$

$$A_P^o = \left(\zeta_p \frac{\Delta x}{\Delta t}\right) \tag{20}$$

$$B = S^{\Phi}\Delta x = \left(\frac{S_P^o - S_P}{\Delta t}\right)\Delta x \tag{21}$$

C) Boundary points (control volume np-1)

In this case, there is a boundary flux (Φ'') that must be replaced according to the existing boundary condition, which is described by Eq. (4). In this way, the equation for the internal points is as follows:

$$\left(\zeta_P \Phi_P - \zeta_{P^O} \Phi_P^o\right)\frac{\Delta x}{\Delta t} = \Phi'' - \Gamma^{\Phi}\left(\frac{\Phi_P - \Phi_S}{\delta x_s}\right) + S^{\Phi}\Delta x \tag{22}$$

The Eq. (4) written as a function of the variable Φ is represented as follows:

$$L\frac{\partial \Phi}{\partial t} = -\Gamma^{\Phi}\left.\frac{\partial \Phi}{\partial x}\right|_n \tag{23}$$

For the boundary flux, the Eq. (23) is discretized, obtaining the following expression:

$$L\left(\frac{\Phi_n - \Phi_n^o}{\Delta t}\right) = -\Gamma_n^{\Phi}\left(\frac{\Phi_n - \Phi_P}{\partial x_n}\right) \tag{24}$$

Thus, we have:

$$\Phi_n = \left(\frac{\frac{L}{\Delta t}\Phi_n^o + \frac{\Gamma_n^\Phi}{\delta x_n}\Phi_P}{\frac{L}{\Delta t} + \frac{\Gamma_n^\Phi}{\delta x_n}} \right) \tag{25}$$

Since that $L\frac{\partial C}{\partial t} = -D\frac{\partial C}{\partial x} = \Phi''$, the expression for the boundary flux is as follows:

$$\Phi'' = \frac{\frac{\Gamma_n^\Phi}{\delta x_n}\left(\Phi_P - \Phi_n^o\right)}{1 + \frac{\Gamma_n^\Phi \Delta t}{\delta x_n L}} \tag{26}$$

In this way, replacing the expression (26) in (22) and rearranging the terms, the following equation for the boundary points is obtained:

$$\mathrm{A_P\Phi_P = A_S\Phi_S + A_n^o\Phi_n^o + A_P^o\Phi_P^o + B} \tag{27}$$

where,

$$A_P = \left(\zeta_P \frac{\Delta x}{\Delta t} + \frac{1}{\frac{\delta x_n}{\Gamma_n^\Phi} + \frac{\Delta t}{L}} + \frac{\Gamma_s^\Phi}{\delta x_s} \right) \tag{28}$$

$$A_S = \left(\frac{\Gamma_s^\Phi}{\delta x_s} \right) \tag{29}$$

$$A_n^o = \left(\frac{1}{\frac{\delta x_n}{\Gamma_n^\Phi} + \frac{\Delta t}{L}} \right) \tag{30}$$

$$A_P^o = \left(\zeta_p \frac{\Delta x}{\Delta t} \right) \tag{31}$$

$$B = S^\Phi \Delta x = \left(\frac{S_P^o - S_P}{\Delta t} \right) \Delta x \tag{32}$$

The Eq. (10), (17) and (27) applied at each control volumes form a system of equations whose solution indicates the concentration of free solute within the solid during the water absorption process.

- Concentration of solute entrapped

To obtain the equations related to the concentration of solute entrapped in the solid, the Eq. (2) in integrated in volume and time as follows:

$$\int_x \int_t \frac{\partial S}{\partial t} dt dx = \int_x \int_t (\lambda C - \mu S) \tag{33}$$

resulting in:

$$\left(S_P - S_P^o\right)\frac{\Delta x}{\Delta t} = \left(\lambda C_P - \mu S_P\right)\Delta x \tag{34}$$

Reorganized the terms of Eq. (33) we obtain the following equation, valid for all points of the control volume:

$$A_P S_P = A_P^o S_P^o + B \tag{35}$$

where,

$$A_P = \left(\frac{\Delta x}{\Delta t} + \mu \Delta x\right) \tag{36}$$

$$A_P^o = \left(\frac{\Delta x}{\Delta t}\right) \tag{37}$$

$$B = \lambda \Delta x C_P \tag{38}$$

- Total moisture content

The total moisture inside the material in a specific position x and instant t is found from the sum of the amounts of free and entrapped solute in accordance with the following equation:

$$M = S + C \tag{39}$$

- Average moisture content

The average moisture content of the solid at any instant of time is given by:

$$\overline{M} = \frac{1}{V}\int M dV = \frac{1}{2a}\int_{-a}^{a} M dx = \frac{1}{a}\int_0^a M dx \tag{40}$$

where, V corresponds to the volume of the solid.

The equation (40) in the discretized form is written as follows:

$$\overline{M} = \frac{1}{a}\sum_{i=2}^{np-1} M \Delta x \tag{41}$$

where np represents the total number of nodal points.

To solve the equation system, a computer code was developed on the *Wolfram Mathematica*® platform. The equations were solved iteratively using the Gauss-Seidel

method, where it was assumed that the numerical solution converged when, from the initial condition, the following convergence criterion was satisfied, at each point of the domain, at a certain time:

$$\left|\Phi_P^{n+1} - \Phi_P^n\right| \leq 10^{-10} \tag{42}$$

where n represents the nth iteration at each instant.

For obtain the predict results, a time step and mesh refinement study was done. After this process we choice a grid with 20 nodal points and a time step $\Delta t = 20$s.

2.4 Validation of the model

The formulation was applied to the moisture diffusion process in polymeric composites reinforced with Caroá fibers. The composite studied have very large width and length compared to the thickness. Then, the pure water penetrates only in the direction of the thickness.

For the validation of the model, the numerical result of the average moisture content was compared with analytical results reported by Santos et al. (2016) and the experimental data reported by Silva (2014) for polymer composite materials reinforced by Caroá fiber. Table 1 presents the geometric parameters used in the simulation.

Table 1. Geometrical parameters used in the simulation

Parameter	Value
L (m)	0.3
a (m)	0.015

Santos et al. (2016) compared the analytical and experimental data of the average moisture content along the transient process. From this comparison, it was estimated the mass diffusion coefficient and the probabilities μ and λ, of the model, using the least squares error technique, given by the following equation:

$$ERQM = \sum_{i=1}^{n} \left[\overline{M}_{predicted} - \overline{M}_{experimental}\right]^2 \tag{46}$$

where n is the number of experimental points. According to the authors, an average quadratic error of 0.047467 ($kg_{water}/kg_{drysolid}$) was obtained. The estimated data are shown in Table 2.

Table 2. Physical parameters used in the simulation

Parameter	Value
D (m^2s^{-1})	$7.020x10^{-12}$
μ (s^{-1})	$1.697x10^{-6}$
λ (s^{-1})	$0.836x10^{-6}$

3 RESULTS AND DISCUSSION

Figure 3 illustrates the comparison between numerical, analytical and experimental data of the average moisture content obtained during water absorption in Caroá fiber reinforced polymer composites at 25°C. The numerical results depend strongly on the boundary conditions, thermo-physical properties and the geometry considered. The observed discrepancies between experimental and numerical data can be attributed to the lack of suitable boundary conditions for the model and the consideration of constant properties. However, from the analysis of the graph it can be observed that the numerical results showed a good agreement between the predict and analytical and experimental results, which shows that the mathematical model presents an adequate description of the diffusion process inside the material.

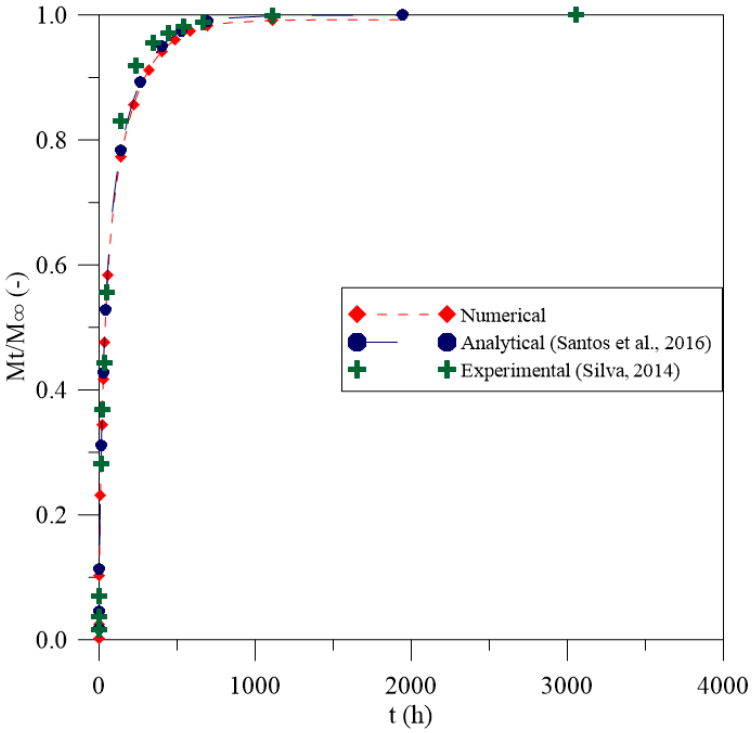

Figure 3. Numerical, analytical and experimental average moisture content of polymer composites reinforced with Caroá fiber during the water absorption process.

Water absorption is facilitated when polymer molecules have clusters capable of forming hydrogen bonds. Plant fibers are rich in cellulose, hemicellulose and lignin which have hydroxy groups, i.e., have high affinity for water. The absorption of water by the resin, in turn, can be considered practically null, since it presents a considerable hydrophobic character (Sanchez et al., 2010). The addition of the plant fibers to the resin generates an increase in the water absorption levels, so an important parameter to be analyzed is how much water is being absorbed by the material over time.

Figure 4 shows the graph obtained for the kinetics of water absorption in the material. The results were plotted as a function of a dimensionless parameter $F_o=Dt/(R+1)a^2$, so called modified Fourier number for mass transfer, aiming a more general mathematical analysis.

From the analysis of the graph it is possible to observe that the water sorption is fast in the initial stages up to a certain modified Fourier number for mass transfer of approximately Fo ≅ 4 and tends to decrease for long exposure times until reaching the equilibrium point (saturation condition $M_\infty = 14.488\%$), where the average moisture content tends to 1. The time to reach the hygroscopic equilibrium was estimated at approximately Fo ≅ 10.

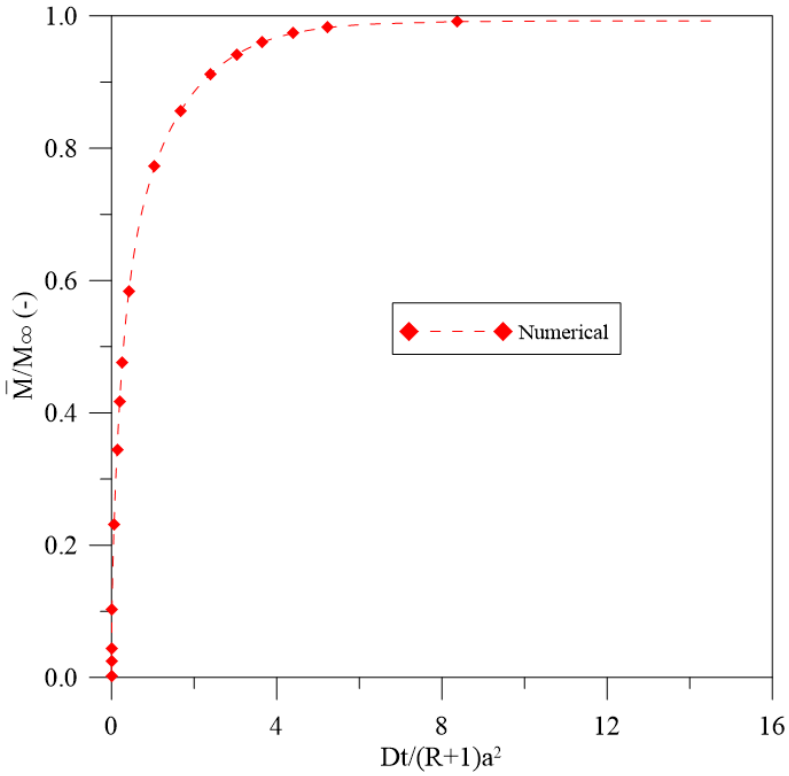

Figure 4. Average moisture content dimensionless as function of the modified Fourier number of mass transfer

Figure 5 shows the graph of the total moisture present in to the material, obtained by the sum of the number of free molecules to be diffused and the number of molecules trapped along its thickness. In regions near the surface, water absorption is faster, as there is a larger area in direct contact with water. The water penetrates the interior of the material generating a higher concentration gradient along the thickness and decreasing with the increase in the immersion time. Thus, at any point inside the solid, the moisture content increases with time until it reaches its equilibrium condition, ie its saturation point. It is intuitive to say that with a longer immersion time there is an increase in the amount of molecules trapped within the material while decreasing the amount of free molecules to diffuse. For a better understanding of this phenomenon, Figures 6 and 7 illustrate the behavior of free and trapped water in the material along the water absorption process.

Figure 6 shows the graph of the variation of free solute concentration along the thickness of the solid, given by the C/Ce, where Ce (estimated as Ce=0.09778) represents the equilibrium concentration of the solute in the fluid medium. Analyzing Figure 6, it is found that, for short times, the concentration variation is large near the surface of the material with a greater amount of free molecules to diffuse in the composite, that is, there is a high concentration gradient of free water in this region. With increasing time, this relationship

tends to approach 1, reaching the hygroscopic equilibrium (saturation), due to the greater water absorption.

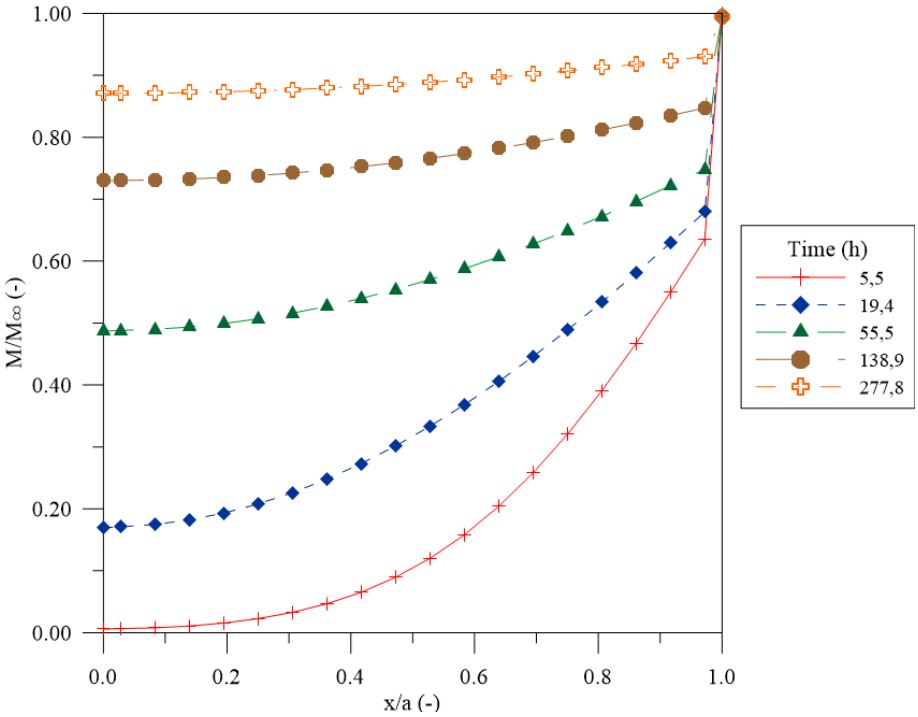

Figure 5. Moisture content present inside polymeric composite reinforced by Caroá fiber along thickness.

.

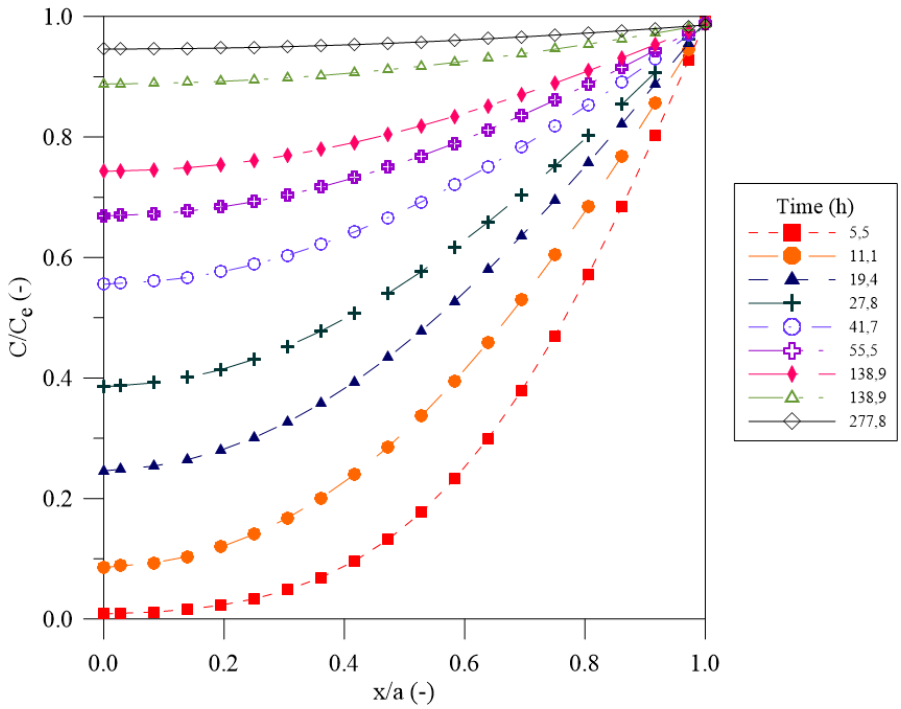

Figure 6. Free solute concentration distribution along the material for different instants of the water absorption process

Figure 7 shows the plot of the variation of the water molecules entrapped along the thickness of the material. Based on the analysis of this graph, it is possible to observe that the increase in the content of trapped molecules depends on the increase in the concentration of free molecules inside the material. The major water concentration gradients are found near the solid surface. For larger times or when there is a greater amount of free molecules inside the material will have a large number of trapped molecules, and this occurs until the equilibrium condition provided in Eq. (5).

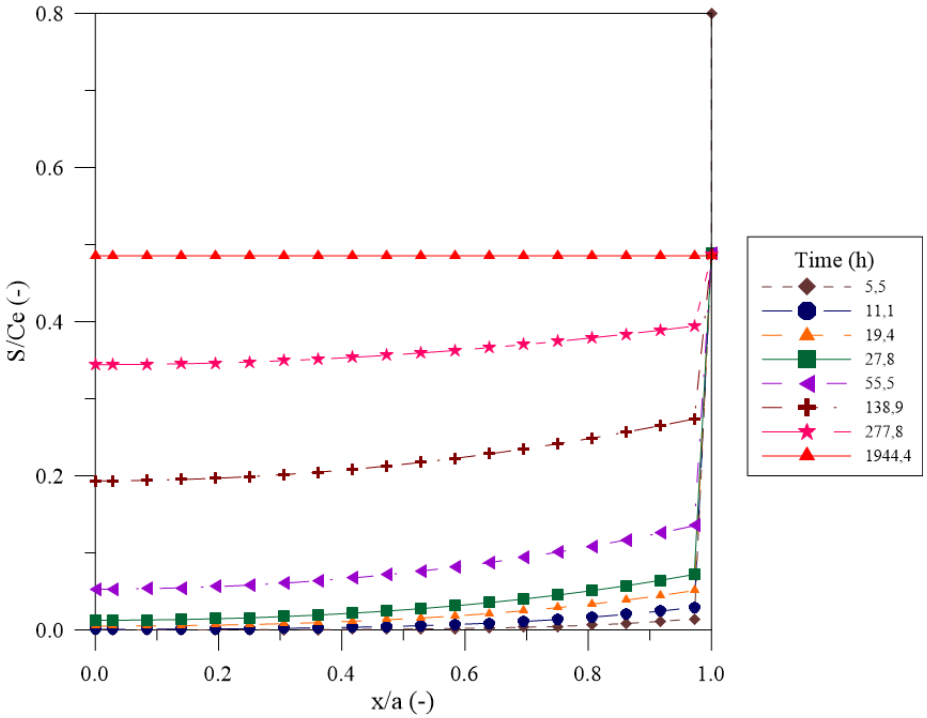

Figure 7. Trapped solute concentration distribution along the material for different instants of the water absorption process.

4 CONCLUSIONS

The mathematical model used describes properly the diffusion of water inside the composite materials, since the numerical solution obtained showed good agreement with the experimental and analytical data of humidification of polymeric composites reinforced with Caroá fiber. From the analysis of the predicted results, it was concluded that the water absorption is fast in the initial stages and tends to decay for long exposure times to water until reaching the equilibrium point. The concentration gradients are higher at the surface of the material and the higher the concentration of the free solute, the higher the concentration of immobilized solute found inside the polymer composite.

Acknowledgements

The authors thanks to CNPq, CAPES and FINEP for financial support and the authors of the references cited in text which helps in the improvement.

REFERENCES

Carvalho, L. H.;Canedo, E.L.; Neto, S.F.;Lima, A.G.B. Moisture Transport Process in Vegetable Fiber Composites: Theory and Analysis for Technological Applications. *In:Industrial and Technological Applications of Transport in Porous Materials.* Springer Berlin Heidelberg, p. 37-62, 2013.

Carter, H. G.; Kibler, K. G. Langmuir-type model for anomalous moisture diffusion in composite resins. *Journal of Composite Materials,* v. 12, n. 2, p. 118-131, 1978.

Cunha, J. A. P.; Costa, M. L.; Rezende, M. C.. Influência de diferentes condições higrotérmicas na resistência à tração de compósitos de fibra de carbono/epóxi modificada. *Polímeros.* v. 16, n. 3, p. 193-201, 2006.

Cruz, V. C. A., Nóbrega, M.M.S., Cavalcanti, W.S., Carvalho, L.H., Lima, A.G.B. Absorção de água em compósitos macambira/poliéster insaturado: um estudo experimental. *VI Congresso Nacional de Engenharia Mecânica. Associação Brasileira de Engenharia e Ciências Mecânicas – ABCM.* Campina Grande, 2010.

Glaskova, T. I.;Guedes, R.M.; Morais, J.J.; Aniskevich, A.N. A comparative analysis of moisture transport models as applied to an epoxy binder. *Mechanics of Composite Materials,* v. 43, n. 4, p. 377-388, 2007.

Joshi, S. V.; Drzal, L. T.; Mohanty, A. K.; Arora, S. Are natural fiber composites environmentally superior to glass fiber reinforced composites?. *Composites Part A: Applied science and manufacturing,* v. 35, n. 3, p. 371-376, 2004.

Mohammed, L.; Ansari, M. N.; Pua, G.; Jawaid, M.; Islam, M. S A review on natural fiber reinforced polymer composite and its applications. *International Journal of Polymer Science,* v. 2015, 2015.

Omrani, E.; Menezes, P. L.; Rohatgi, P. K. State of the art on tribological behavior of polymer matrix composites reinforced with natural fibers in the green materials world. *Engineering Science and Technology, an International Journal***,** v.47, p.777-780, 2015.

Patel, H.; Parkhe, A.; Shrama, P. K. Mechanical Behaviors Of Banana And Sisal Hybrid Composites Reinforced With Epoxy Resin. *International Journal of Research – Granthaalayah,* Vol. 4, n. 1,p.206-216, 2016.

Santos, W. R. G., Melo, R. Q. C., Lima, A. G. B. Water Absorption in Polymer Composites Reinforced with Vegetable Fiber Using Langmuir-Type Model: An Exact Mathematical Treatment, *Defect and Diffusion Forum*, Vol. 371, pp. 102-110, 2016.

Silva, C.J. *Absorção de água em materiais compósitos de fibra vegetal: modelagem e simulação via CFX*. Dissertação (Mestrado). Centro de Ciências e Tecnologia. Universidade Federal de Campina Grande. Campina Grande, 2014.